Design of a Low Voltage DC Microgrid Based on Renewable Energy to be Applied in Communities where Grid Connection is not Available

Raimon Padrós-Valls, Eduardo Iraola-de-Acevedo, Eduardo Prieto-Araujo, Oriol Gomis-Bellmunt CITCEA-UPC
Avda. Diagonal, 647, 08028, Barcelona, Spain
Email: {eduardo.prieto-araujo, oriol.gomis}@upc.edu

***Abstract*—This article compares different topologies for Low Voltage DC networks that might be used in the electrification process of communities without access to electricity. These type of networks usually include distributed generation (mainly PV), energy storage (batteries) and loads in several houses. Currently, these grids are being built isolated from the AC network and without including any power converter to control the power flow. A comparison between the typical converter-less approach and three alternative topologies is developed, one including a DC/DC converter connected to the central battery, another including converters connected to the PV generation systems, and a third one including converters connected to each generation and storage system.**

I. Introduction

Currently, an electrification process is being developed in communities without access to electricity. In certain areas, such systems are being built combining distributed generation, mainly solar Photovoltaic (PV), energy storage (batteries) and households loads interconnected in a simple and affordable manner, using a Low Voltage (LV) DC network [1]. These grids are being constructed without including any power converters, neither to perform the connection to the AC network, nor to control the power flow inside the DC network. Having a converter-less network, reduces the initial investment cost but it might limit its operation and performance during the project lifetime.

In this article, the converter-less grid topology is compared with three additional topologies. The first additional topology only includes a converter that is able to control the power injected/absorbed by the energy storage system, the second option includes a converter connected to the output of each generation system to control the power injected to the network, and the third option includes a converter connected to each generation and storage system.

A methodology has been developed to compare the four different alternatives, based on the following procedure. First, an equivalent steady-state model of the DC microgrid is obtained for each alternative. Then each DC circuit power flow is solved based on a defined irradiance (maximum and minimum), load (maximum and minimum) and battery voltage conditions. Then, based on the obtained results a comparison of the system overall performance between the different alternatives is developed.

II. System description and modelling

The circuit explored in this article is composed only by batteries, PV panels and loads as shown in Fig. 1(a). To perform the steady-state circuit studies, the nodal analysis method [2] is used to model the entire network. PV cells, batteries and loads are represented as voltage sources and the interconnection cables as resistances (see Fig. 1(b)). In order to simplify the computation, the Norton equivalent is used, as depicted in Fig. 1(c)

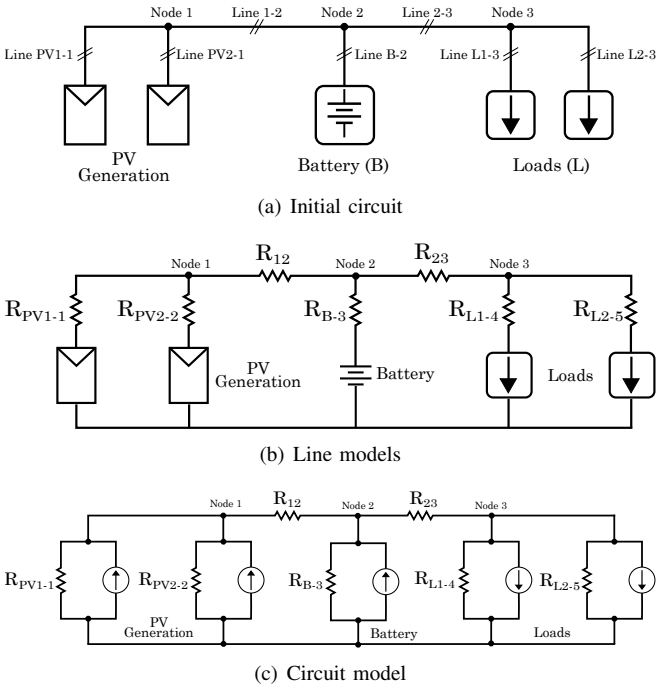

(a) Initial circuit

(b) Line models

(c) Circuit model

Fig. 1. Obtention of the circuit model

Then, a circuit admittance matrix is used to represent the circuit obtained in Fig. 1(c). For a generic circuit, the impedance matrix is

$$\mathbf{Y} = \begin{pmatrix} y_{11} & y_{12} & \cdot & \cdot & y_{1m} \\ y_{21} & y_{22} & \cdot & \cdot & y_{2m} \\ \cdot & \cdot & \cdot & & \cdot \\ \cdot & \cdot & & \cdot & \cdot \\ y_{m1} & y_{m2} & \cdot & \cdot & y_{mm} \end{pmatrix} \quad (1)$$

where the diagonal elements y_{ii} are the sum of the conductances connected to each of the nodes, and the off-diagonal

elements y_{ij} are the conductances between nodes i and j, with a negative sign. Then, the circuit equations can be written as

$$\mathbf{Y} \cdot \mathbf{V} = \mathbf{I} \tag{2}$$

where $\mathbf{V}$ is the node voltage vector and $\mathbf{Y}$ is the node current vector. Using this method, the admittance matrix becomes easy to compute using the cables' resistivity, the different possible sections and the distance between the different nodes.

Having the admittance matrix defined, additional values or equations for either the voltage or current unknown variables should be included into the system. On the one hand, the system consumptions are defined as constant power loads. On the other hand, the representation of PV panels and batteries would vary depending on the type of connection to the network (directly connected or through a converter).

A. PV panel modeling

In this work, a simple model is used to represent the PV cell characteristic curve [3].

$$I = I_L - I_0 \left(exp\frac{q(V + IR_S)}{nkT} - 1 \right) - \frac{V + IR_S}{R_{SH}} \tag{3}$$

$$I_L = (G/G_{ref}) I_{L_{ref}} (1 + \alpha \cdot (T - T_{ref})) \tag{4}$$

where V is the output voltage, I is the output current, I_0 is the diode saturation current, I_L are the photovoltaic current, R_S is the series resistance, R_{SH} is the shunt resistance, G is the solar irradiance, n is the diode quality factor, q is the magnitude of charge carried by an electron, k is the Boltzmann constant, T is the cell temperature and α is the Temperature coefficient.

III. DC GRID TOPOLOGIES

In this paper four different grid topologies are studied. Next, the particularities of each topology and how the power flow analysis is addressed are described in the following sections.

A. Topology 1: Converter-less grid

For the first scenario without converters (see Fig. 1(a)), both the battery voltage and the load power consumption are imposed. Besides, the characteristic $V - I$ curve of the above referenced PV panel model is used to solve the power flow.

B. Topology 2: converters connected to the PV panels

In this scenario each PV cell is connected to the network through a DC/DC converter (see Fig. 2). Using these converters, it is assumed that all PV panels are working at their Maximum Power Point (MPP). Therefore, the system of equations can be straightforwardly solved, as instead of using the characteristic $V - I$ curve from the PV panel, its production can be imposed based on the irradiance. The converter losses are not being considered in the power flow analysis. Also, the battery voltage and the power consumed by the loads are imposed as in the previous case.

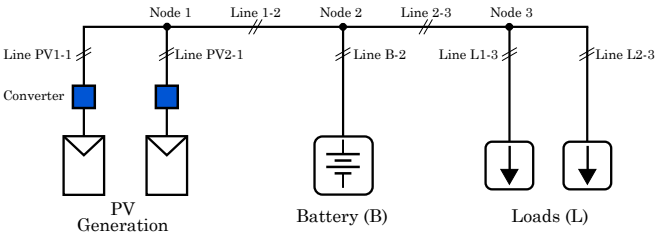

Fig. 2. Grid with converters connected to the PV panels

C. Topology 3: converter connected to the battery

In this case, only the battery is connected to the grid through a DC/DC converter (see Fig. 3). In this situation, the battery DC/DC converter applied voltage is set based on an optimization algorithm that maximizes the power produced by PV panels considering the system circuit losses. The PV panels are modelled using their $V - I$ characteristic curve and ideal converters are assumed.

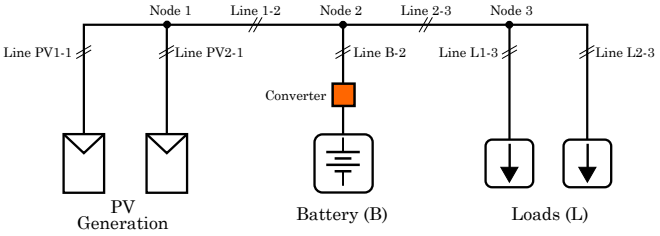

Fig. 3. Grid with a converter connected to the battery

D. Topology 4: converters connected to each PV panel and the battery

The last grid topology is shown in Fig. 4. In this network, a DC/DC converter is connected to each PV panel and battery of the system. In this case, as the PV and battery converters can apply variable voltages, the system maximum voltage constraint handled by the loads becomes relevant, setting a maximum operational limit of the system.

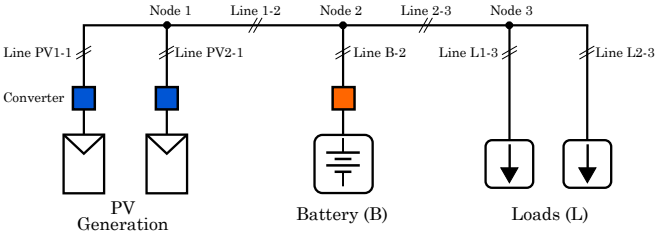

Fig. 4. Grid with converters connected both to the PV panels and the battery

IV. CASE STUDY

A. Microgrid description

In this section, a detailed steady state analysis of a low voltage DC microgrid is performed. The microgrid under study is shown in Fig. 5 and its electrical scheme is represented in Fig. 6. The grid is composed of six photovoltaic panels, one battery and six Tier 2 loads[1] [4].

[1]Low consumption no higher than 50 W and 4 hours a day maximum, as defined by SE4ALL

Photovoltaic panels and circuit parameters are detailed in Table I and Table II respectively. It is assumed that the microgrid location is Dhaka (Bangladesh). Then, the solar PV production is obtained based on this location considering the irradiation and temperature local conditions using NREL software PVWatts [5]. Besides, additional assumptions have been made:

- The PV panel model used is the same for each of the houses
- All the PV cells receive the same irradiance
- The temperature of all the PV cells is equal
- The demand is equal for all the different households
- Grid nominal operation voltage is 12 V
- A load profile has been generated based on Tier 2 consumption data [4]
- The allowed voltage deviation at the loads point of connection is $\pm 25\%$ of the nominal value
- The PV collection circuit and the loads circuit are equal (distances and cable sections)

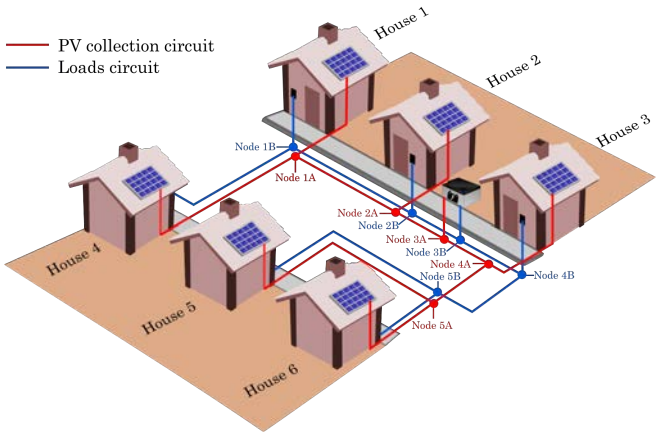

Fig. 5. Drawing of the case study microgrid

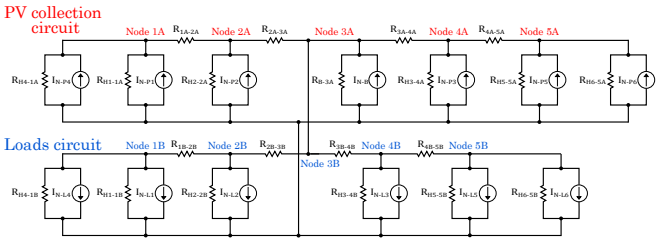

Fig. 6. Scheme from the analyzed microgrid

Based on this information, a comparison of the operation between the four different network topologies is carried out in the following sections.

B. Scenarios studied

In this section, the four topologies presented are compared based on three different generation/load scenarios: full irradiance without load, full load without irradiance, and full irradiance and load. The specific values used for the study are detailed in Table II.

The four topologies are compared in terms of PV power production P_{pv}, battery power exchanged P_{bat}, maximum voltage drop V_{drop} (absolute and percentage), maximum current I_{max} and system losses P_{loss}. Also, for those cases including a converter connected to the battery, its voltage is also included for comparison V_{bat-dc}.

TABLE I
PV CELL PARAMETERS [6]

Parameter	Value	Units
$I_{SC_{ref}}$	1.45	A
V_{oc}	22.2	V
R_S	1.0394	Ω
R_{SH}	2177.3561	Ω
G_{ref}	1000	W/m^2
n	1.3	-
q	$1.6022 \cdot 10^{-19}$	C
k	$1.3806 \cdot 10^{-23}$	J/K
T_{ref}	298.15	K
α	0.0048	C^{-1}
$Ncell$	36	-
I_{Pmax}	1.37	A

TABLE II
PARAMETERS USED FOR THE CASE STUDY

Parameter	Value	Units
Cable section	4	mm^2
Resistivity	0.0171	Ω mm^2/m
Irradiance	1000 (Day) and 0 (Night)	W/m^2
Power per load	50 (full load) and 0 (no load)	W
Battery voltage	12	V
PV cells	6	-
Loads	6	-
Batteries	1	-

1) Results - converter-less grid: The results for this first topology are shown in Table III and Fig. 7. It can be seen that the PV panels work at an approximately 75 % of their nominal production, at full irradiance and full load conditions. Additionally, at full irradiance and no load conditions, Table III reveals that the power produced by the PV panels is similar to the full load and full irradiance case. Moreover, it can be stated that the losses represents approximately a 16 % of the power consumed when the loads are connected.

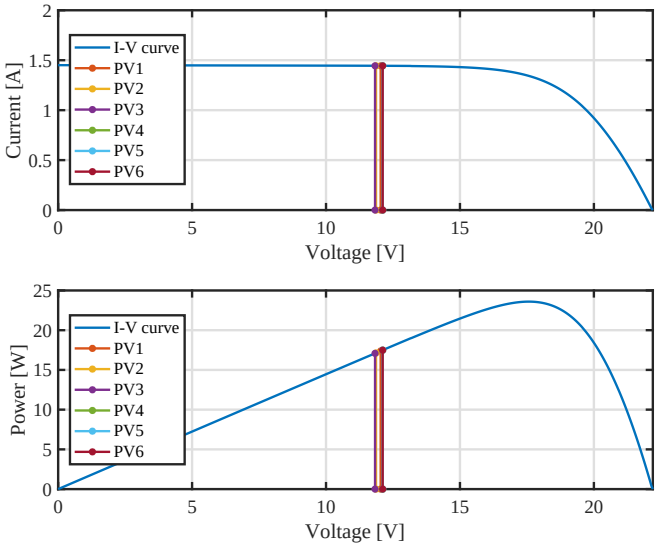

Fig. 7. PV operating points with no converters, full load and full irradiance

TABLE III
POWER FLOW RESULTS - NO CONVERTERS

Parameter Name	$G = 1000$ W/m^2 $P_L = 50$ W		$G = 0$ W/m^2 $P_L = 50$ W		$G = 1000$ W/m^2 $P_L = 0$ W	
	Sum	Mean	Sum	Mean	Sum	Mean
P_{pv}	104.06 W	17.34 W	0 W	0 W	108.24 W	18.04 W
P_{load}	-300 W	-50 W	-300 W	-50 W	0 W	0 W
P_{bat}	240.7 W	240.7 W	350.66 W	350.66 W	-103.43 W	-103.43 W
Max V_{drop}	12.61 %	-	13.02 %	-	3.54 %	-
I_{max}	20.06 A	-	29.22 A	-	8.619 A	-
P_{loss}	44.76 W	-	50.66 W	-	4.34 W	-

2) Results - Converters connected to the PV panels: The results for this topology are shown in Table IV. When there is no irradiance, the results are not included, as they are equal to the converter-less topology. As expected, there is an improvement of the system performance as all the PV cells are operating at the MPP. However, it can be seen that the system losses are still high as in the previous case.

TABLE IV
POWER FLOW RESULTS - PV CONVERTERS

Parameter Name	$G = 1000$ W/m^2 $P_L = 50$ W		$G = 1000$ W/m^2 $P_L = 0$ W	
	Sum	Mean	Sum	Mean
P_{pv}	141.57 W	23.60 W	141.57 W	23.60 W
P_{load}	-300 W	-50 W	0 W	0 W
P_{bat}	203.22 W	203.22 W	-134.32 W	-134.32 W
Max V_{drop}	12.47 %	-	4.54 %	-
I_{max}	16.94 A	-	11.19 A	-
P_{loss}	44.79 W	-	7.25 W	-

3) Results - Converter connected to the battery: The results for this scenario are shown in Table V and Fig. 8. With this topology the system losses are reduced up to a 67% compared to the previous cases, and the PV cells are producing almost at the MPP.

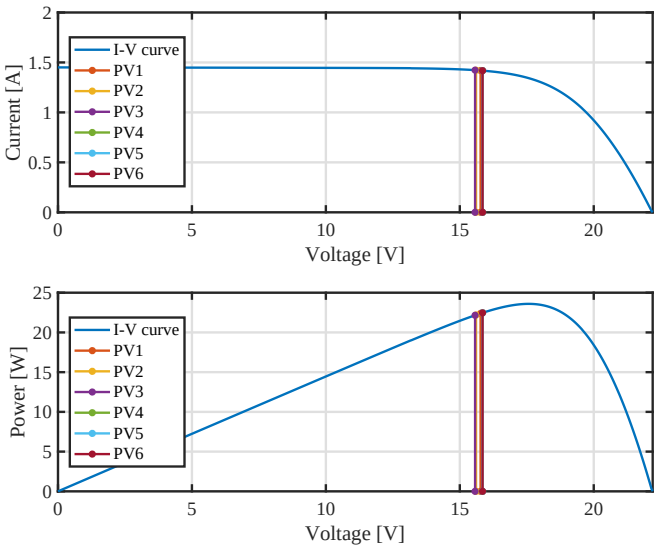

Fig. 8. PV operating points with battery converter, full load and full irradiance

4) Results - Converters connected to each PV panel and the battery: The results for this last case are shown in Table VI. As it is expected, there is an operational improvement compared to the previous cases, in terms of losses and power production by the PVs. The results for the no irradiance case are equal to the ones obtained for the Battery converter case.

TABLE V
POWER FLOW RESULTS - BATTERY CONVERTER

Parameter Name	$G = 1000$ W/m^2 $P_L = 50$ W		$G = 0$ W/m^2 $P_L = 50$ W		$G = 1000$ W/m^2 $P_L = 0$ W	
	Sum	Mean	Sum	Mean	Sum	Mean
P_{pv}	134.15 W	22.36 W	0 W	0 W	131.33 W	21.88 W
P_{load}	-300 W	-50 W	-300 W	-50 W	0 W	0 W
P_{bat}	189.06 W	189.06 W	325.01 W	325.01 W	-127.00 W	-127.00 W
Max V_{drop}	6.77 %	-	6.77 %	-	2.84 %	-
I_{max}	12.11 A	-	20.64 A	-	8.55 A	-
P_{loss}	23.21 W	-	25.02 W	-	4.26 W	-
V_{bat-dc}	15.61 V	-	15.75 V	-	14.85 V	-

TABLE VI
POWER FLOW RESULTS - PV AND BATTERY CONVERTERS

Parameter Name	$G = 1000$ W/m^2 $P_L = 50$ W		$G = 1000$ W/m^2 $P_L = 0$ W	
	Sum	Mean	Sum	Mean
P_{pv}	141.57 W	23.60 W	141.57 W	23.60 W
P_{load}	-300 W	-50 W	0 W	0 W
P_{bat}	181.77 W	181.77 W	-136.65 W	-136.65 W
Max V_{drop}	6.77 %	-	3.05 %	-
I_{max}	11.65 A	-	9.21 A	-
P_{loss}	23.34 W	-	4.92 W	-
V_{bat-dc}	15.60 V	-	14.84 V	-

C. Results discussion

Comparing the four topologies, it can be stated that the one including converters connected to the PV panels and battery is the most efficient one. It is capable of maximizing the power production of the PV panels (operating at MPP) while reducing the system losses. An interesting alternative is the topology including a single converter connected to the battery, as it operates the PV panels close to the MPP while reducing importantly the system losses. This topology becomes interesting as no converters are required for the PV panels, thus reducing the initial hardware investment cost of the installation. The converter-less topology is also an interesting alternative as it is able to extract a 75% of the nominal power of the PV panels. However, the associated losses are considerably higher compared to the alternatives including a converter connected to the battery. Regarding the topology including converters connected to the PV panels, it is able to maximize the power extraction from the PV panels, but it is not capable of reducing the associated system losses.

Then, it can concluded that an additional technical-economic analysis must be carried out, combining the developed study with a capital and maintenance cost analysis of each installation, in order to see which of the alternatives is the most interesting for each community.

D. Microgrid day simulation

Assuming that the selected alternative is the most complete network topology (including converters connected to the PV panels and the battery in Fig. 5 grid) a time domain simulation of the system throughout a day is carried out. The solver is executed each hour during one day, imposing the hourly consumptions (based on [4]) and the hourly irradiance and temperature for Dhaka, Bangladesh (based on PVWatts [5]). The results are shown in Fig. 9, showing 24 hours of a day of February. Note that, the battery capacity and its stored energy are not included the simulation.

It can be seen that the PV panels can cover the 100% of the Tier 2-based electrical demand, of course assuming that the system includes a battery able to absorb the PV produced energy during the day.

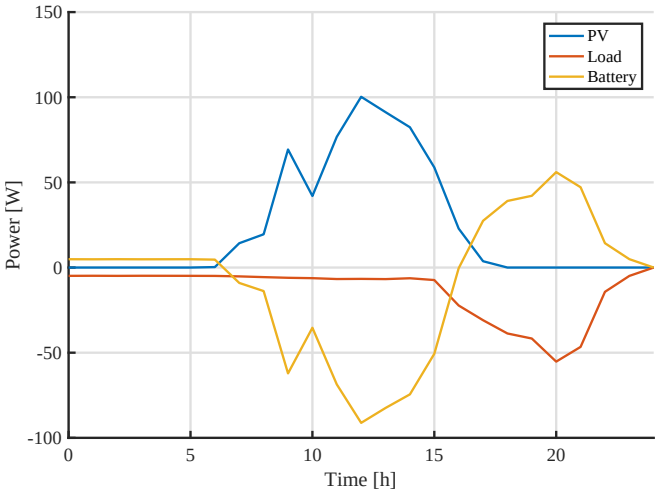

Fig. 9. Evolution of the power delivered by each group of elements during a day

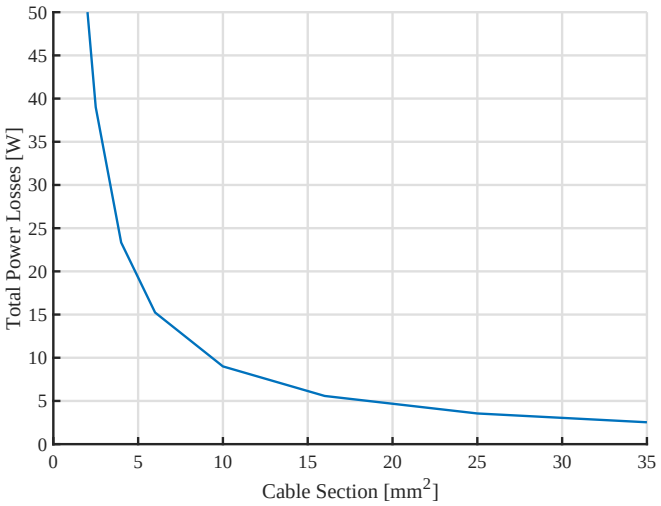

Fig. 10. System power losses for different cable sections

E. Comparison of different wire sections

A further analysis of the cable section impact on the system losses is carried out for the most complete network topology (including converters connected to the PV panels and the battery in Fig. 5 grid). The losses are compared for cable sections ranging between 2.5 and 35 mm^2. The analysis is performed for full load and full irradiance conditions. Results are shown in Table VII and Fig. 10.

It can be seen that increasing the cable section, starting from the lower end (2.5-6 mm^2), can be interesting in terms of losses, as an important reduction can be achieved. On the contrary, for large cable sections (20-35 mm^2) the loss reduction achieved is much lower. As in previous cases, it would be interesting to combine this analysis with a technical-economic study, introducing the cost of the cable.

TABLE VII
LOSSES BETWEEN DIFFERENT CABLE SECTIONS

Section [mm^2]	Total Loss [W]
2.5	39.01
4	23.34
6	15.24
10	9.00
16	5.58
25	3.55
35	2.53

V. CONCLUSION

A comparison between four different topologies for Low Voltage DC networks that might be used in the electrification process of communities without access to electricity has been presented. These microgrids are usually being built connecting PV panels, energy storage and loads without using converters. This alternative has been compared to three additional topologies: one connecting converters to each PV panel, another connecting a converter to the battery and third one connecting converters to the PV panels and the battery. The study has shown that the alternative including converters connected to the PV panels and the battery achieves a better overall operation of the system maximizing the PV production while reducing the system losses, as expected. Also, the alternative including a single converter connected to the battery has been found particularly interesting, as it is able to maintain the PV panels operating close to the MPP while reducing the system losses. In order to decide which is the most suitable topology for a certain community, further technical-economic studies should be developed combining the electrical analysis shown and the cost of installation and maintenance of the converters.

ACKNOWLEDGMENT

This work has been funded in part by the Spanish Ministry of Economy and Competitiveness under Project ENE2015-67048-C4-1-R. This research was co-financed by the European Regional Development Fund (ERDF). The authors would also like to thank José Luis Román for supporting this study.

REFERENCES

[1] S. Groh, J. van der Straeten, B. E. Lasch, D. Gershenson, W. Leal Filho, and D. M. Kammen, *Decentralized Solutions for Developing Economies*. Springer, 2015.
[2] P. Dimo, "Nodal analysis of power systems," 1 1975.
[3] G. Walker, "Evaluating MPPT converter topologies using a MATLAB PV model."
[4] Sustainable Energy for All. Beyond connections: Energy access redefined. [Online]. Available: http://www.se4all.org/sites/default/files/Beyond-Connections-Introducing-Multi-Tier-Framework-for-Tracking-Energy-Access.pdf
[5] NREL. Estimation of energy production and cost of energy of grid-connected. [Online]. Available: http://pvwatts.nrel.gov/ [Accessed: Jan. 13, 2018]
[6] ENF Solar. Blue solaria 25 wp 18.2 v solar panel. [Online]. Available: https://es.enfsolar.com/pv/panel-datasheet/Polycrystalline/28543